

## DNA Extension in Nanochannels

Leon Dean

Chemical Engineering, University of Texas at Austin

NNIN REU Site: Nanofabrication Center, University of Minnesota-Twin Cities, Minneapolis, MN

NNIN REU Principal Investigator: Kevin Dorfman, Chemical Engr. and Materials Science, University of Minnesota-Twin Cities

NNIN REU Mentor: Julian Sheats, Chemical Engineering and Materials Science, University of Minnesota-Twin Cities

Contact: leondean@utexas.edu, jtsheat@umn.edu, dorfman@umn.edu

### Abstract:

Confining deoxyribonucleic acid (DNA) in nanochannels is an effective method for achieving the elongation necessary for DNA barcoding. Recent simulations have shown that semiflexible polymers like DNA exhibit different confinement behavior than flexible polymers in intermediate channel sizes. The purpose of this study is to measure the fractional extension of lambda DNA ( $\lambda$ -DNA) as a function of nanochannel width in a range of channel sizes and to compare the experimental results to the aforementioned simulation results. Several nanofluidic devices containing arrays of nanochannels were fabricated, and preliminary extension measurements were made. The results should improve theoretical understanding of the dynamics of single DNA molecules confined in nanochannels.

### Introduction:

DNA barcoding has emerged as a useful technology for high-throughput genome mapping, but requires a method for elongating individual DNA molecules. The two most common elongation methods are molecular combing [1] and channel confinement [2]. Understanding DNA confinement behavior is critical for the accurate assessment of the locations of fluorescently-labeled probes along confined DNA molecules.

All polymers can be characterized by contour length ( $L$ ), the length of a fully extended chain, persistence length ( $l_p$ ), a measure of backbone stiffness, and effective width ( $w$ ). For a confined polymer, the channel width ( $D$ ) is also an important parameter. Channel width has a profound effect on extension ( $X$ ), which is the observed length of the confined polymer chain. For the dyed  $\lambda$ -phage DNA used in this experiment,  $L \approx 21 \mu\text{m}$ ,  $l_p \approx 53 \text{ nm}$ , and  $w \approx 4.6 \text{ nm}$  [3].  $D$  can be replaced by the geometric mean of the channel depth and width [4].

The theory explaining mean fractional extension ( $\langle X \rangle / L$ ) as a function of  $D$  is well-defined for flexible polymers.

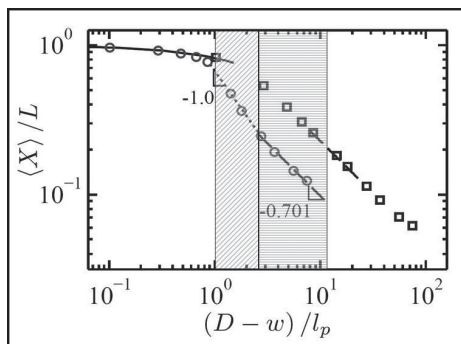


Figure 1: Log-log plot of fractional extension versus effective nanochannel width from simulation for a semiflexible polymer (circles) and a flexible polymer (squares). Adapted with permission from [5].

In the weak confinement regime, corresponding to larger values of  $D$ , the scaling law is derived from de Gennes blob theory. In the strong confinement regime, corresponding to smaller values of  $D$ , the scaling law is derived from Odijk deflection theory [3]. However, recent Monte Carlo simulations have shown that additional confinement regimes exist between the de Gennes and the Odijk regimes for semiflexible polymers like DNA [3, 5]. Figure 1 illustrates how semiflexible polymers exhibit behavior different from flexible polymers in the shaded transition regimes. The given

slopes correspond to the exponents for the scaling laws in the respective regimes.

### Experimental Procedure:

Experimental measurements within the additional regimes were performed in nanofluidic devices fabricated on silicon substrates. Each device contained a nanochannel array between two parallel microchannels with reservoirs for loading. The nanochannel array was patterned by electron beam lithography, which controlled the widths of the channels, followed by reactive ion etching, which controlled the depth of the channels. The microchannels and reservoirs were patterned by contact photolithography and etched with a deep Bosch process. Access holes were cut into the reservoirs with a wet potassium hydroxide etch, while the rest of the device was protected by a film of silicon nitride. A silicon oxide layer of  $\sim 200 \text{ nm}$  was thermally grown to provide electrical insulation. All devices were anodic-bonded to fused silica in order to enclose the channels. Resulting devices contained nanochannels with  $D$  between 50 and 500 nm. Nanochannel lengths were either 1 mm or 100  $\mu\text{m}$ . Figure 2 shows a nanochannel before bonding.

The device was filled with 2.2X TBE (tris, borate, ethylenediaminetetraacetic acid) aqueous buffer containing  $\beta$ -mercaptoethanol (5% w/w) and ascorbic acid (0.07% w/w) to suppress bleaching, as well as polyvinylpyrrolidone

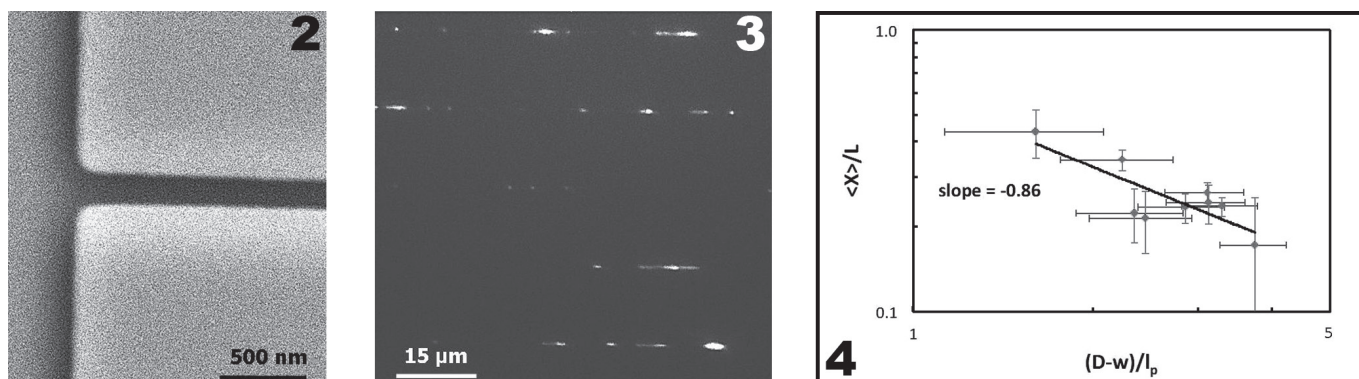


Figure 2, left: SEM of the entrance of a nanochannel with dimensions of  $180 \text{ nm} \times 160 \text{ nm}$ .

Figure 3, middle: Optical micrograph of fluorescently dyed  $\lambda$ -DNA molecules inserted into nanochannels.

Figure 4, right: Log-log plot of fractional extension versus effective nanochannel width from experiment for dyed  $\lambda$ -DNA. Horizontal error bars represent instrument uncertainty and vertical error bars represent the standard deviation of multiple measurements.

(0.07% w/w) to prevent sticking of the DNA. It was found that the nanochannels with shorter lengths filled spontaneously by capillary action, while the nanochannels with longer lengths typically required pre-filling with a lower surface tension fluid like ethanol [6].

The  $\lambda$ -DNA, dyed with YOYO-1, was inserted into a reservoir and pumped through a microchannel. Then electrophoresis was applied across the nanochannels to force some DNA molecules into nanochannels. Optical microscopy images were taken with a  $100\times$  oil immersion objective under fluorescent light.

### Results and Conclusions:

Figure 3 shows a representative image of DNA successfully inserted into nanochannels. The figure includes fragmented molecules resulting from photocleavage or shear cleavage. Other regions contained agglomerations of stuck DNA molecules which did not respond to an electric field.

After the fragmented and stuck DNA molecules were removed as outliers, the rest of the elongated DNA molecules were analyzed. For each molecule, a threshold intensity value was established and the length of the intensity profile above that threshold was measured. Typically,  $\sim 100$  measurements were obtained for each molecule and averaged into a mean extension.

Figure 4 shows a plot of mean fractional extension versus effective channel width. The exponent of the power law regression is  $-0.86$ , which closely corresponds to previous research [4] and lies in between the simulation exponents of  $-1.0$  and  $-0.701$  for the two additional regimes.

The number of experimental data points is insufficient to make further conclusions.

### Future Work:

Additional extensions measurements will be gathered at many different channel sizes in order to fill more data points into Figure 4. In conjunction with reduced uncertainty, this will allow the determination of experimental scaling laws for fractional extension as a function of channel width as well as any transition points within the additional confinement regimes.

### Acknowledgments:

The author thanks Dr. Julian Sheats and Prof. Kevin Dorfman, along with the University of Minnesota Nanofabrication Center staff, for help throughout the project. The author also thanks the NNIN REU Program and the NSF for financial support.

### References:

- [1] Michalet, X. et al. *Science*, 277, 5331, 1518-1523 (1997).
- [2] Lam, E.T. et al. *Nature Biotechnology*, 30, 771-776 (2012).
- [3] Wang, Y., Tree, D.R., and Dorfman, K.D. *Macromolecules*, 44, 6594-6604 (2011).
- [4] Reisner, W. et al. *Physical Review Letters*, 94, 196101 (2005).
- [5] Tree, D.R., Wang, Y., and Dorfman, K.D. *Physical Review Letters*, 108, 228105 (2012).
- [6] Han, A., et al., *J. of Colloid and Interface Science*, 293, 151-157 (2006).